AERODYNAMIC NUMERICAL/EXPERIMENTAL COMPARISON OF A HYPERSONIC TEST VEHICLE IN MORE&LESS PROGRAM

P. Roncioni[1], M. Marini[1], R. Fusaro[2], N. Viola[2], D. Pepelea[3], B. Cakir[4], M. Clay[5]

[1]CIRA - Centro Italiano Ricerche Aerospaziali - Italy
[2]POLITO - Politecnico di Torino - Italy
[3]INCAS - National Institute for Aerospace Research, Romania
[4]VKI, Von Karman Institute, Belgium
[5]REL – Reaction Engine Ltd, United Kingdom

Abstract

This paper deals with a numerical and experimental activity for the development and integration of the aerodynamic database of hypersonic test vehicle in the framework of the H2020 More&Less project. At this purpose, a dedicated methodology has been developed and applied to several supersonic/hypersonic vehicles. This methodology foresees the development of aerodynamic databases by means of incremental steps starting from simplified methods up to very reliable data based on high-fidelity CFD simulations and experimental measurements with associated confidence levels. In particular, in this paper a direct comparison between CFD results and experimental measurements is reported being this a fundamental step for the building of the final aerodynamic database of the Mach 5 flying experimental vehicle.

Keywords: Aerodynamic Characterization; CFD, Experimental Measurements, Hypersonic civil transport, MORE&LESS

1. Introduction

The European Commission is funding the H2020 MORE&LESS Project (MDO and REgulations for Low boom and Environmentally Sustainable Supersonic aviation) ([1]), aiming at developing a wide design platform for future supersonic aviation on the base of global environmental regulations. A multi-disciplinary optimization framework to assess the holistic impact of supersonic aviation onto environment is foreseen that can incorporate high-fidelity modelling activities and test campaigns. At first, different disciplines will tackle separate design topics through modelling and tests and then the environmental impact of these aircraft concepts will be evaluated through the holistic framework.
To further extend the validity of theories and models, the entire spectrum of supersonic speed regime ranging from Mach 2 to Mach 5 is considered. Moreover, the analysis is not only restricted to aircraft using traditional hydrocarbon fuels, but it moves beyond, addressing aircraft concepts exploiting alternative fuels, such as biofuels and cryogenic fuels. The idea of considering more case-studies with different configurations, performance and fuels fosters the enhancement of the flexibility of the tools, which, starting from the case-studies, are developed based on modelling activities and test campaigns as products that can be flexible enough to be applied to several future vehicle concepts. In order to achieve this aim one important activity is the development of the aerodynamic database. This paper deals with the development and integration of increasing-fidelity aerodynamic modelling approaches in the conceptual design of hypersonic cruisers. This methodology foresees the development of aerodynamic databases (i.e., aerodatabases) by means of incremental steps starting from simplified methods (panels methods and/or low fidelity CFD simulations) up to very reliable data based on high fidelity CFD simulations and experimental measurements with associated confidence levels. This allows us to follow the development phases of the vehicle all along the entire design cycle by providing preliminary aerodynamic coefficients at initial conceptual approach, and therefore

very tailored aerodatabases at advanced design phases.
A fundamental step of this procedure is the direct comparison of numerical and experimental data before to proceed to the final assembling of the aerodatabase conceived as nominal values and uncertainties error bars. In this paper this activity is focused on the Reaction Engine Ltd. (REL) Hypersonic Test Bed (HTB) experimental vehicle, a Mach 5 aircraft whose main aim is the in-flight experimentation of the SABRE engine.

2. CS2 Vehicle Description

The reference geometry CS2 (Case Study 2, i.e. CS-2) to be studied is the Hypersonic Test Bed (HTB) vehicle concept currently under investigation by Reaction Engines Ltd.. The HTB is intended to serve as a flying demonstrator or "test bed" for SABRE – the Synergetic Air-Breathing Rocket Engine – which is under development at Reaction Engines Ltd. SABRE is set to revolutionise space access and hypersonic flight by enabling reusable, aircraft-like launch vehicles, and unique high-Mach propulsion technologies. The HTB also presents an important opportunity for commercial hypersonic research, serving as an experimental test platform for novel airframe and engine technologies.
Figure 1 illustrates the geometry of the vehicle currently being used for this study. As indicated, the vehicle features two propulsion systems:

- An experimental air-breathing engine, situated in a nacelle mounted on the upper fuselage
- A rocket engine, found housed inside the rear end of the fuselage

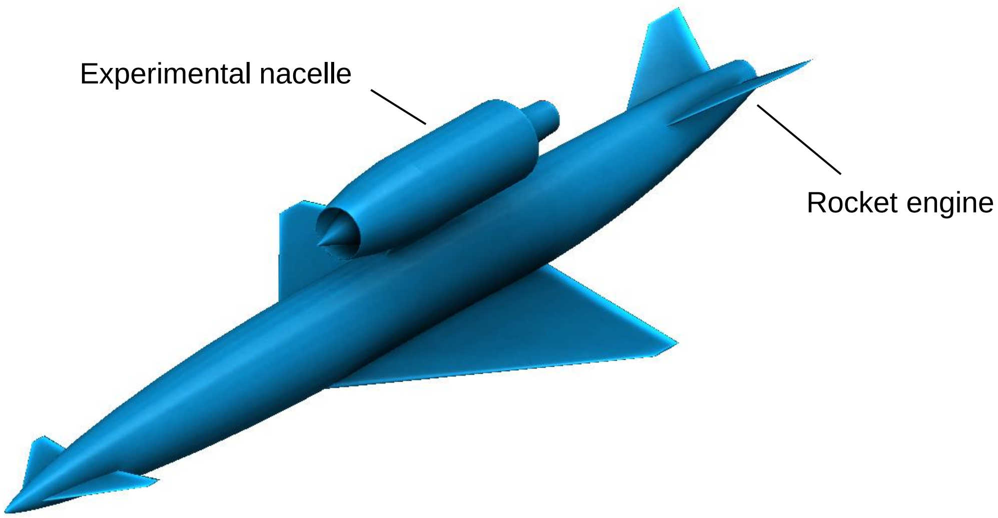

Figure 1 - HTB geometry.

The reference geometrical properties are:

Flight full configuration	INCAS WT (1:28)
L_{ref} = 24.534 m	L_{ref} = 0.876214 m
S_{ref} = 40.7751 m^2	S_{ref} = 0.052009 m^2
Moment Reference Point = Nosetip	

The coefficients for the forces and moments are normalized as:

$$C_{Force} = \frac{Force}{Q * S_{ref}}$$

$$C_{Moment} = \frac{Moment}{Q * S_{ref} * L_{ref}}$$

The reference system is the one used for CFD simulations as shown in Figure 2, for which:

- The origin is located at the nosetip,
- The x-axis is directed from nose to base,
- The y-axis is directed toward the right (as right wing),
- The z-axis is such to form a right-handed reference system (from bottom to up).

In order to use the classical aeronautical reference system (see Figure 3) it must be changed the direction of x and z axes, and also the signs of rolling and yawing moments (coefficients C_l and C_n). The angle of sideslip (AoS or β) is positive if the wind comes from the right of the vehicle, thus meaning that for a positive AoS the y-component of velocity is negative. In the following the formulas for the three velocity components (α or AoA is the angle of attack):

$$u = \cos\alpha \cos\beta$$
$$v = -\sin\beta$$
$$w = \sin\alpha \cos\beta$$

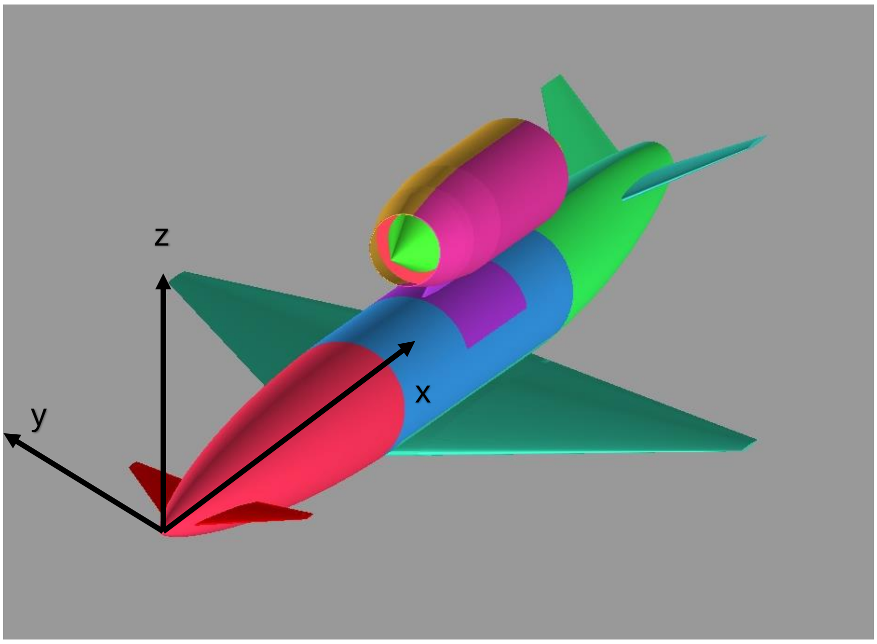

Figure 2 - CS-2. CFD Reference System.

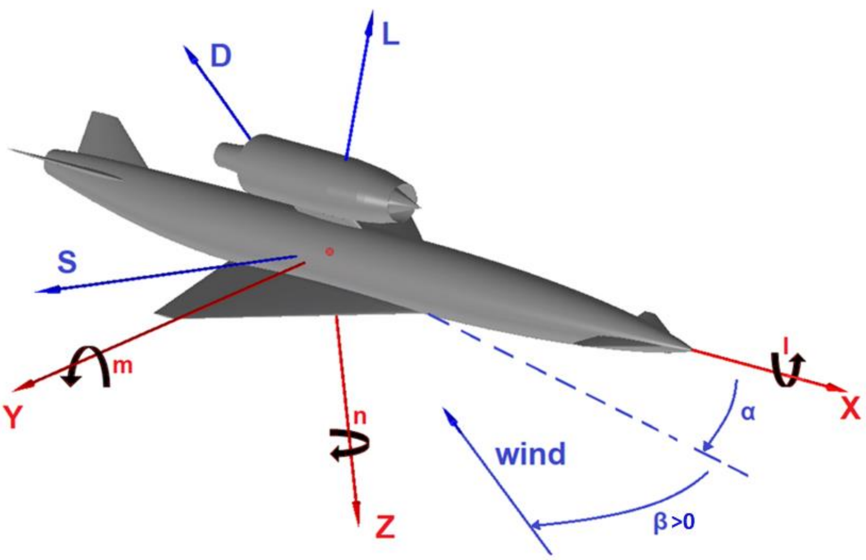

Figure 3 - CS-2. Aeronautical Body and Wind Reference Systems.

3. CFD Aerodynamic Activity

For CS2 vehicle both wind tunnel tests and CFD simulations are foreseen in order to build a reliable aerodynamic database with suitable uncertainty levels. The experimental campaign is foreseen at INCAS (Mach = 0.4 -> 3.5) and VKI (M=5.0) high-speed wind tunnels on different models.
In Figure 4 is reported the REL HTB geometry for which the activity is focused on. Based on the experience gained in the H2020 STRATOFLY project, inviscid CFD simulations are used on the clean configuration and then viscous effects corrections are applied ([3]). These corrections can be estimated through engineering formulations, which are widely available in literature and whose factors can be eventually tuned to the current vehicle configuration.

Figure 4 – REL HTB geometry.

The viscous effect engineering formulation ([12] [13] [14]) can be generalized as it follows:

$$(\Delta C_D)_{visc_{ext}} = \alpha * \frac{1}{[Log(Re)]^{2.58}} * \frac{1}{(1+\beta * M^2)^{\gamma}} * \frac{A_{wet}}{A_{ref}}, \quad (1)$$

The parametric formulation reported in Eq. (1) allows for the estimation of the viscous effect by correcting the turbulent flat plate theory (represented by the term $\frac{1}{[Log(Re)]^{2.58}}$, see [12]) with (i) the factor $\frac{1}{(1+\beta * M^2)^{\gamma}}$ which takes into account the compressibility effect ([13]), (ii) the wetted and the reference areas ratio and (iii). The parameters α, β, γ shall be customized depending on the vehicle configuration. For example, the values $\alpha = 0.43, \beta = 0.31$ and $\gamma = 0.37$ have been found for STRATOFLY MR3 configuration.
The general formulation is synthetized in the following formulations (for the longitudinal flight and body axis reference frame), where the nominal coefficients are obtained as a summation of several contributions: clean configuration, control surfaces deflection, viscous effects and thrust effects:

$$C_N = (C_N)_{clean} + \sum_{i=1}^{n} (\Delta C_N)_i$$

$$C_A = (C_A)_{clean_{inv}} + (\Delta C_A)_{visc_{ext}} + (\Delta C_A)_{visc_{int}} + \sum_{i=1}^{n} (\Delta C_A)_i$$

$$C_{My} = (C_{My})_{clean} + \sum_{i=1}^{n} (\Delta C_{My})_i + (\Delta C_{My})_{Thrust}$$

The viscous correction is applied only to the axial coefficient and is considered constant with the angle of attack, in this way pitching moment and normal force are unaffected. The lift and drag coefficients are obtained by projecting the body forces on the wind axis reference system (Figure 3) by means of the following formulas (longitudinal case):

$$C_L = C_N * \cos\alpha - C_A * \sin\alpha$$

$$C_D = C_N * \sin\alpha + C_A * \cos\alpha$$

A particular attention must be given to the engine treatment. Since the internal flow process, including the combustion phenomenon, is not simulated not being the scope of the present work and also not being necessary for the evaluation of the numerical database, a particular attention is thus given to the engine boundary condition treatment by means of suitable inflow/outflow numerical settings. Another aspect to be considered is the position of the inlet spike that varies with the Mach number (Figure 5), in such a way to accommodate efficiently the external shocks pattern.

Mach	Position	
	Cowl radii	metres
0.0 – 2.0	1.370	0.723
2.5	1.675	0.884
3.0	1.897	1.002
3.5	2.063	1.089
4.0	2.189	1.156
4.5	2.287	1.208
5.0	2.363	1.248
5.5	2.425	1.280

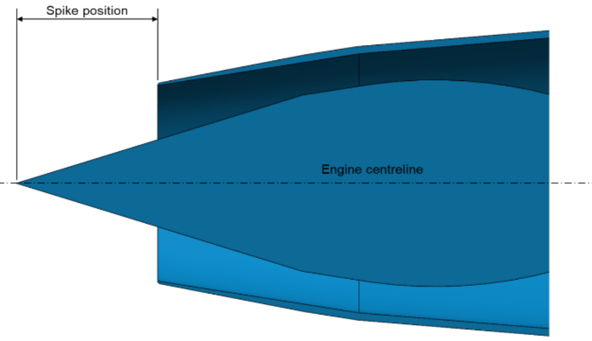

Figure 5 – Spike position.

Several unstructured grids on the full-body of about 7.5 million (supersonic) and 10 million (subsonic) of cells have been generated by means of ICEMCFD-TETRA (Figure 6) software, and the CFD simulations have been conducted by using ANSYS-FLUENT code in the hypothesis of inviscid flow.

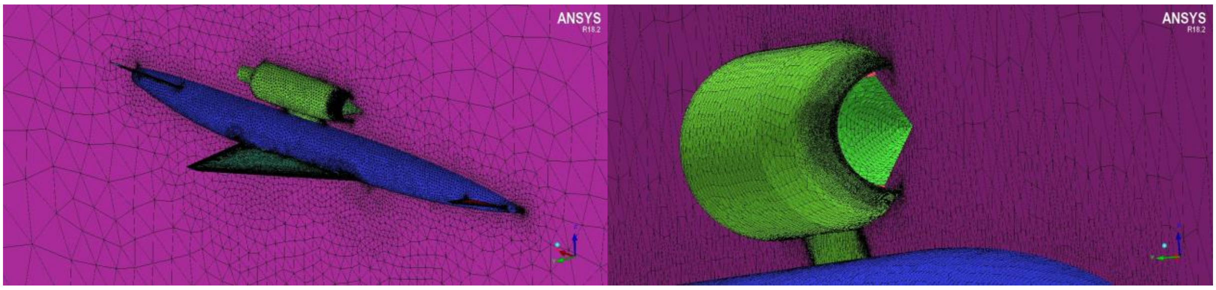

Figure 6 - CS-2. Eulerian Grid. 7.5 million cells on full-body.

In the following figures (Figure 7) the Mach number contours at an angle of attack of 20° are reported. Large expansion and recompression zones are predicted over the wing and fuselage. It can be noted as the shock in front of the inlet spike is well swallowed by the nacelle, and the shocks of the nacelle impinge over the top fuselage creating an overpressure zone (Figure 8).

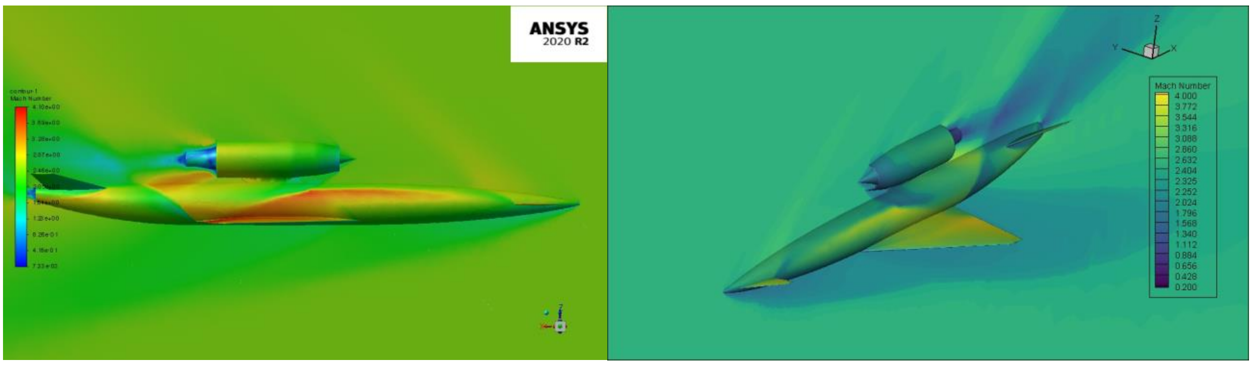

Figure 7 - CS-2, Mach number contours at M=2.5, AoA=20°, AoS=0°. Side view (left) and isometric view (right).

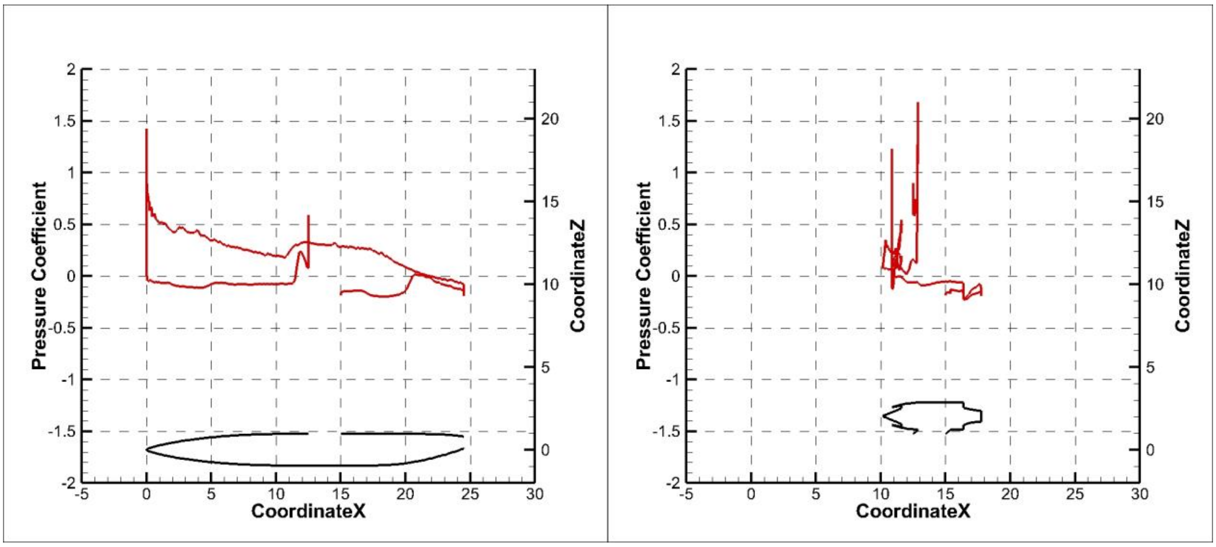

Figure 8 - CS-2. Cp distribution at Y=0m. In black: fuselage (left) and nacelle (right).

The whole clean aerodatabase all along the Mach number and angle of attack ranges is reported in the following figures in terms of global aerodynamic coefficients.

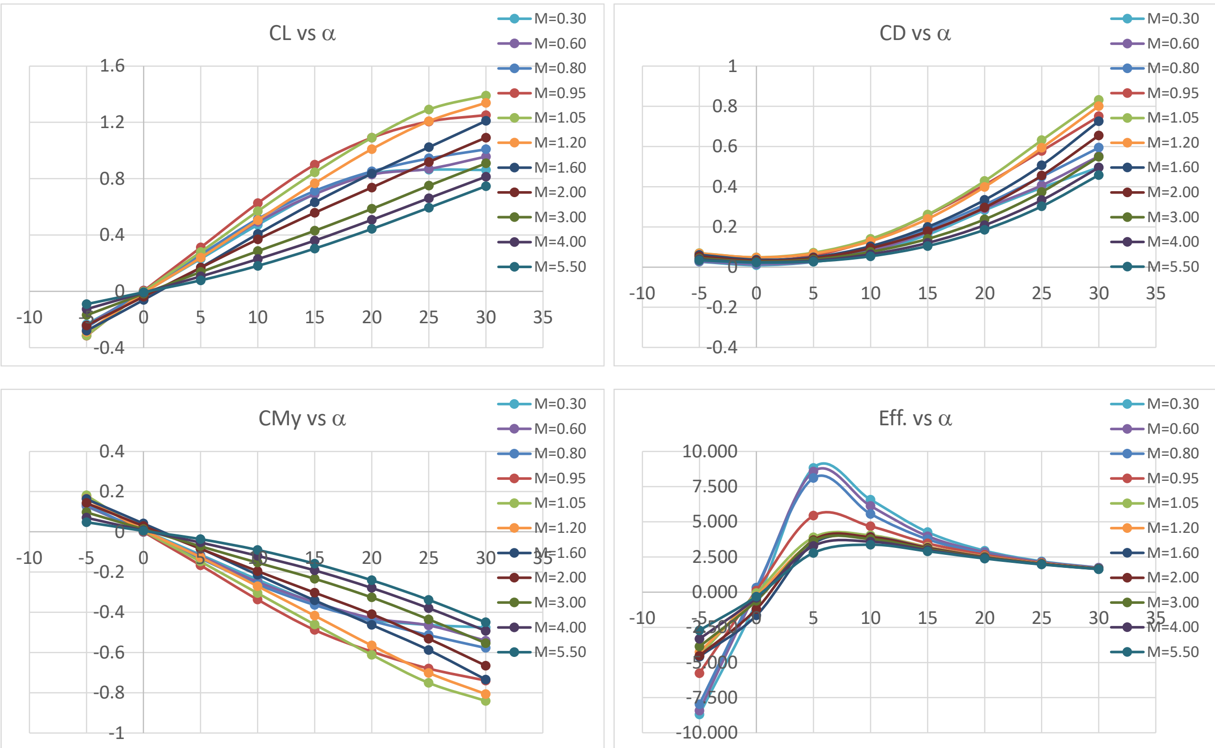

Figure 9 – Whole Aerodatabase. Clean Configuration.

A different behaviour can be observed for subsonic and supersonic regimes. The stall phenomenon starts at an angle of attack of 20 deg at M=0.3, whereas in supersonic range a quasi-linear trend seems to continue for higher angles of attack (mainly due to vortex lift). A characterization of the control surfaces effect and the analysis of trimmability and stability have also been done but not reported here for the sake of brevity.

4. Experimental Activity Description

The experimental activities have been conducted at VKI for the Mach 5 specific condition and at INCAS Trisonic Facility for the 0.4-3.5 Mach number range. In the following subsections a short description of the dedicated apparatus is given.

4.1 Aerodynamic testing at VKI WT Facility

The tests are conducted at the H3 hypersonic facility of von Karman Institute. The VKI-H3 wind tunnel (Fig. 10) is a low enthalpy, blow-down facility designed to generate hypersonic flows at large Reynolds numbers [14]. For the present investigations, its operational capabilities are extended with the addition of a newly designed and integrated axisymmetric contoured nozzle producing a uniform Mach 5 free jet with an inviscid diameter of 120 mm [16]. Dried air is supplied from a pebble-bed heater at stagnation pressures from 7 to 16bar at stagnation temperatures ranging from 350K to 550K. The free-stream unit Reynolds number may be varied from 5x106 to 35x106/m with the current Mach 5 nozzle [17]. Run times up 30 seconds of wind tunnel operation with the model injected can be achieved. Utilizing the institute wide compressed air generation and storage systems, tests up to 10 times can be made with the nominal operating stagnation pressure of 13bars.

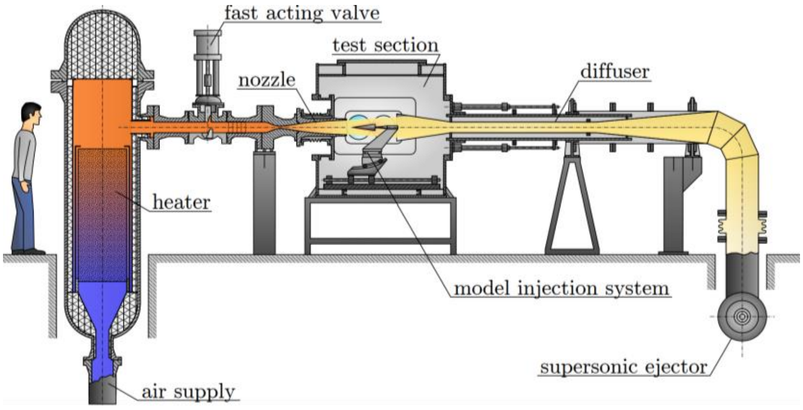

Figure 10 – Schematic representation of the VKI-H3 hypersonic blowdown wind tunnel.

The testing article referred to as the hypersonic test bed for flight testing of high-speed propulsion systems (Fig.11, left) is designed by Reaction Engines Ltd. for the purpose of conducting flight tests with engines such as Scimitar [18] and SABRE [19]. The wind tunnel model employed for the current study is a 1:129 scaled down and modified version of this vehicle. While the original vehicle is fitted with a rocket engine within the fuselage and a supersonic engine sitting on top of the vehicle, the present aerodynamic investigations are focusing exclusively on the aerodynamics of the main airframe, excluding the supersonic engine nacelle. The wind tunnel model is sting-mounted within the test section using the rocket exhaust. (Fig.11, middle & right). Hence, the model tested is composed of a Sears–Haack body of 14mm external diameter and 180.6mm length. The model has stationary control surfaces of canards, central belly mounted wings and a V-tail to act as a combined vertical and horizontal stabilizer.

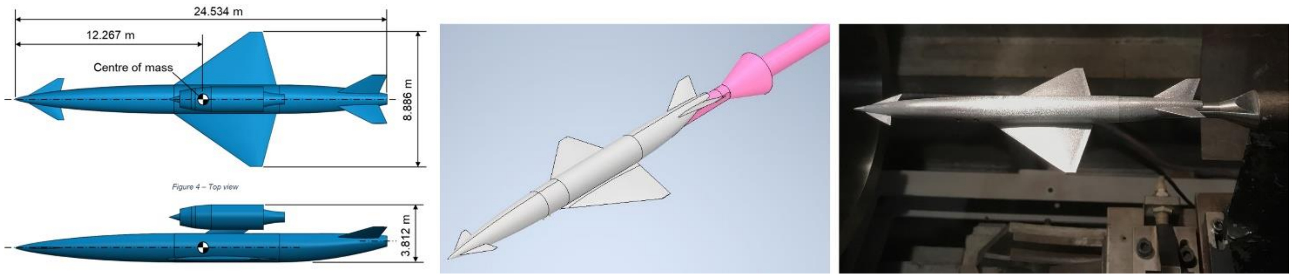

Figure 11 – Scaled wind tunnel model sizing based on the optimized geometric specifications.

For the experimental testing campaign of REL-HTB at Mach 5, a 3-components internal strain gauge balance is designed. It aims at measuring simultaneously the drag force, lift force and pitching moment acting on the vehicle. In order to define the static range of the balance, a preliminary estimation of the forces expected at Mach 5 (longitudinal and normal) and moment (pitching) is performed using the in-house code ANTARES [20] for different angles of attack. The balance design is severely constrained by the slender configuration of the vehicle and by the effective test rhombus dimensions of the new Mach 5 nozzle which required the balance outer diameter not to exceed 8 mm (Fig.11). The in-house balance fulfils all design requirements and is instrumented with Micro Measurements S5077 strain gauges featuring a general-purpose miniature pattern, and each characterized by a normalized resistance of 350Ω.

4.2 Aerodynamic testing at INCAS WT Facility

A bigger part of the experimental activities for the aerodynamic characterization of the vehicle concept took place at INCAS Trisonic Wind Tunnel. The 1.2m x 1.2m wind tunnel is a blowdown type with a speed range from low subsonic (M=0.4) to a maximum supersonic Mach number of 3.5. This range includes transonic Mach numbers which are obtained through use of a perforated wall called transonic test section.
The test setup used a strain gauge balance for aerodynamic forces and moments and pressure taps for base drag correction. Schlieren system was also installed to acquire flow visualization. A fine layer of carborundum grit (60 μm) was added as transition strip, located on the lower/upper surfaces of the wing (5% wing chord), V-tail (5% of tail chord) and fuselage nose (half the distance between nose and canard root).

Figure 12 – CS-2 model installed on the pitch mechanism.

The scale of the model (Figure *12*) of 1:28 was determined by selecting the suitable balance that meets the requirements in terms of aerodynamic loads and available space for installing it. Due to the complexity of the vehicle configuration the model was designed with a closed nacelle and the results were adjusted afterwards by elaborating CFD-based corrections.

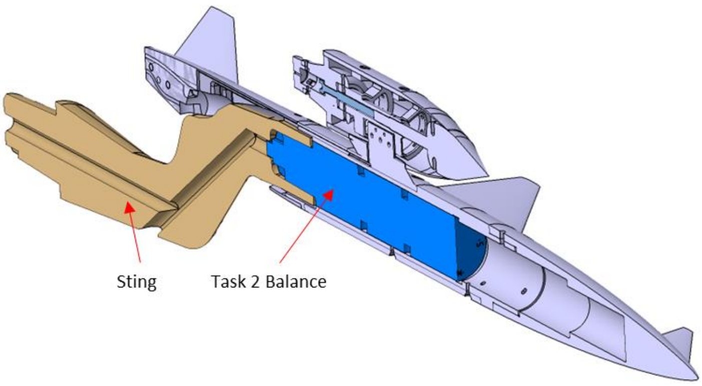

Figure 13 – Cutaway of the wind tunnel model with sting.

Table 1 – Experimental test matrix

M	0.4	0.6	0.8	0.95	1.05	1.1	1.2	1.4	1.6	2	2.5	3.5
Re x 10^6	11.4	15.7	18.7	20.1	20.7	20.8	21	20.7	19.8	18.2	25.2	32.7

The experimental runs were performed to include a broad range of Mach numbers from 0.4 up to 3.5

(Table 1) and relatively large angles off attack (-5:20 deg). A couple of runs were dedicated to study the lateral-directional behaviour by imposing a 10 deg sideslip angle. Aerodynamic test campaign consisted of 28 runs, four of which allowed colour Schlieren visualizations.

5. Experimental/Numerical comparison and aerodatabase generation

The experimental results, conducted at VKI WT for what concerns the Mach 5 cruise conditions and the at INCAS WT for the remaining regimes of flight are reported hereinafter compared to the numerical simulations results with the aim of building a final CS-2 aerodatabase.

At first a numerical rebuilding of VKI test campaign is reported. Figure 14 shows the grids for CFD WT models to be used to calculate engine and sting effects in VKI WT conditions. The comparison has been done step by step starting from the inviscid CFD results and taking into account the viscosity by engineering formulation, and finally with a direct viscous simulation. As can be seen from Figure 15 the direct viscous simulation gives the best comparison, as expected. Good results are also given by inviscid simulations with adding viscous effect at wind tunnel conditions. A good comparison is also evident for the pitching moment coefficient considering that this value is calculated with respect to the centre of mass and is very close to zero.

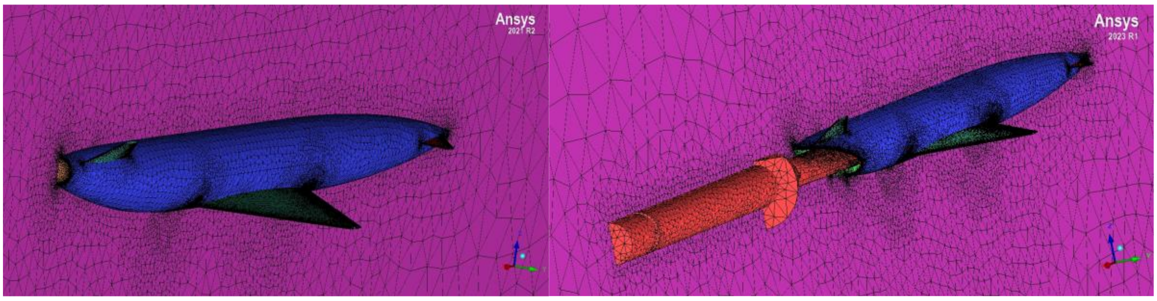

Figure 14 – REL HTB Grids in VKI WT. No Engine on top and without and with sting. Nearly 7.5 M cells.

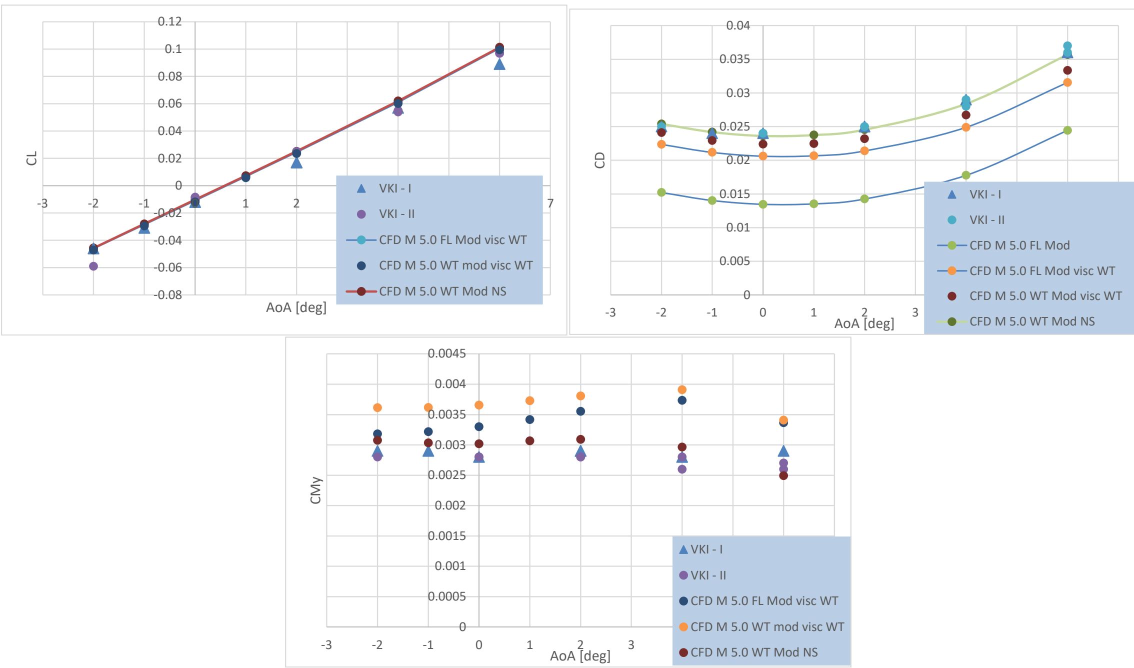

Figure 15 – REL HTB CFD/EXP comparison at VKI WT conditions. M=5.

For INCAS test campaign results a direct comparison in flight conditions is conducted since the experimental results have been provided with WT and Reynolds corrections. Figure 16 shows a comparison for nominal values of aerodynamic longitudinal coefficients (C_L, C_D, C_m) at several Mach numbers. For CFD both inviscid and viscous simulations are reported. The agreement is generally good especially for supersonic cases. In subsonic cases the differences between inviscid and viscous results are more evident, fiving these latter a better agreement with experiments.

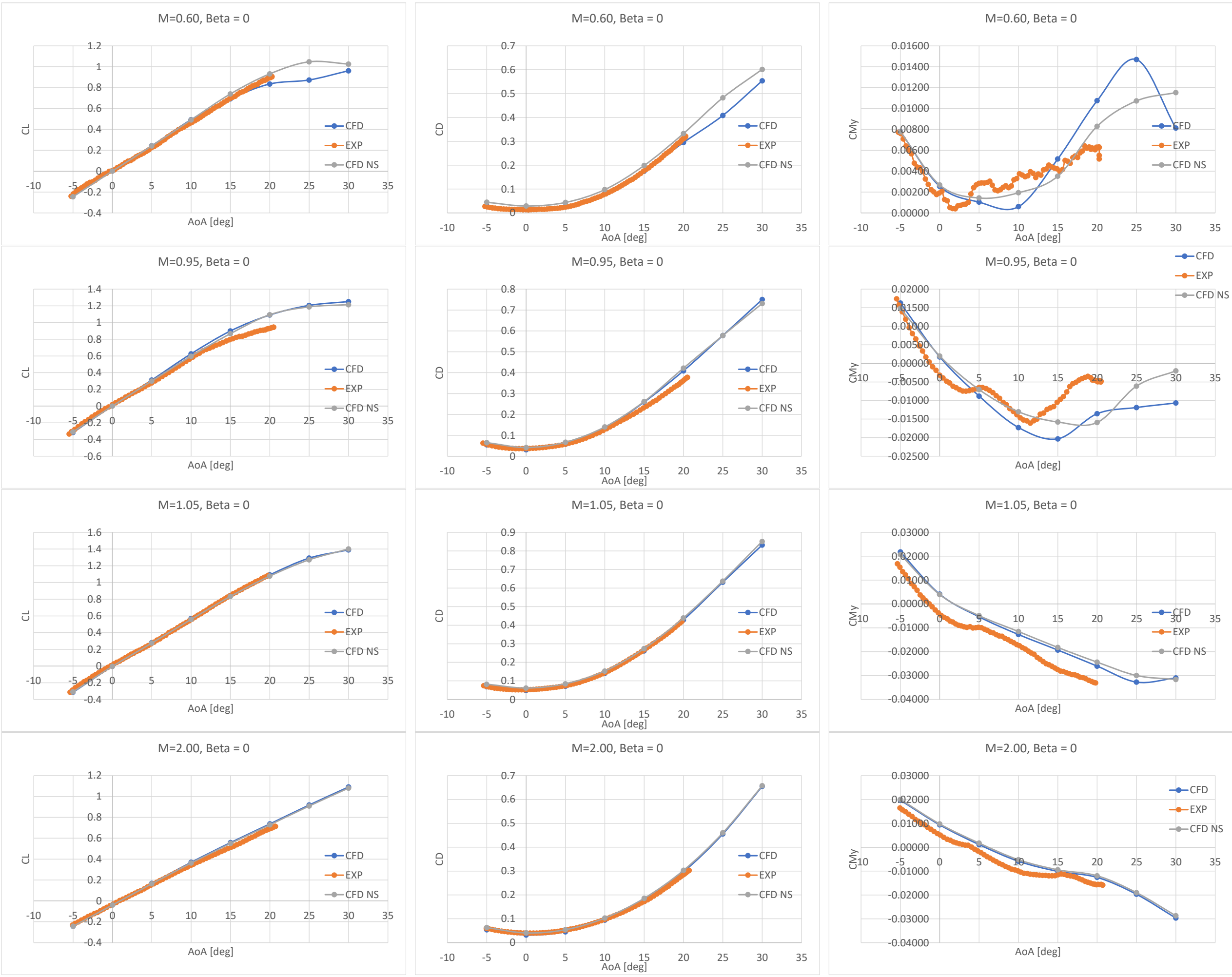

Figure 16 – REL HTB CFD/EXP comparison at INCAS WT conditions. M=0.60, 0.95, 1.05, 2.00.

In order to build the final aerodatabase the error bars must be taken into account. A general prospect of all sources of errors that are usually considered is reported the following table. The terminology is not unique and different terms can be found in literature.

Table 2 – General prospect of all possible source of errors

Uncertainties/ Tolerances	**Dispersions/ Variations**	**Confidence Level/ Error bars**
WT balance **WT corrections**	WT repeatability Difference of WT model and/or testing wrt flight conditions	Summation of Uncertainties and Dispersions
CFD-GRID **CFD-Modeling**	Difference of CFD model and/or running wrt flight conditions	

To show the procedure followed for the generation of the final CS-2 aerodatabase, the case at Mach 1.05 is described. In Figure 17 each set of data contains its own set of uncertainties. The experimental data take into account for repeatability and balance errors, and CFD data for modelling (inviscid vs viscous) and grid sensitivity errors ([11]). In this particular case the other WT source of errors are corrected by means of dedicated CFD simulations (not reported here).

From analysing Figure 17, it is clear the good agreement for C_L and C_D coefficients since each error bar contains the other nominal value, for example each experimental data is fully contained in the numerical error bar. However, there is no intersection of error bars for the pitching moment C_{My}, meaning that the comparison cannot be considered good. In this case, an enlargement of numerical uncertainties is necessary.

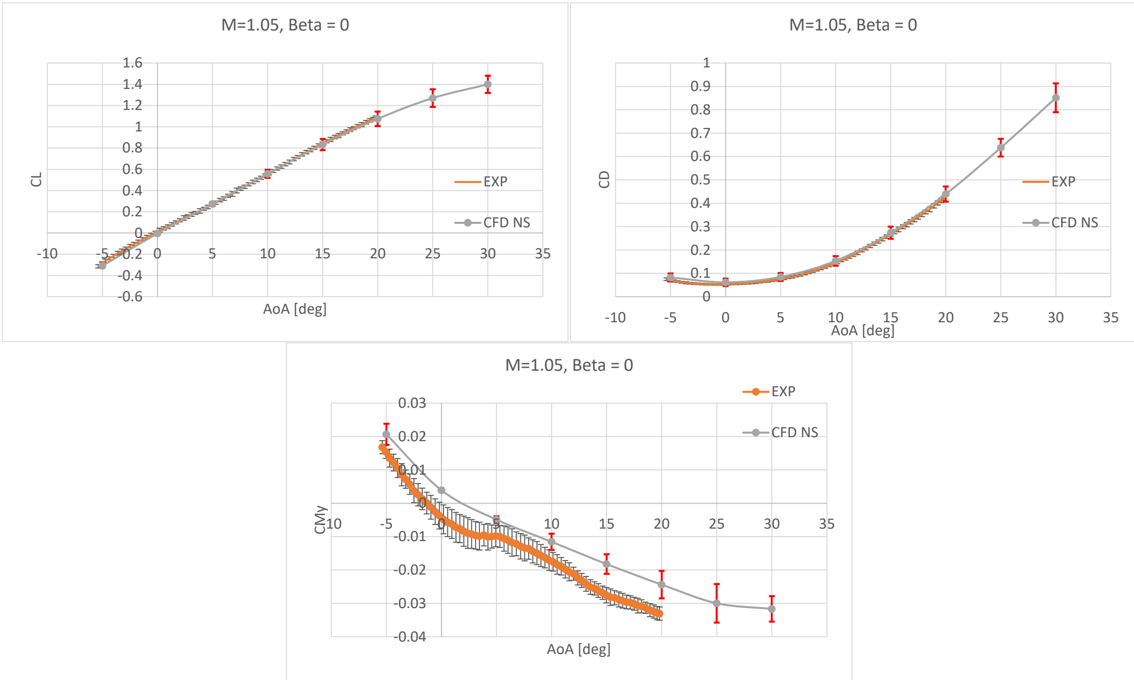

Figure 17 – REL HTB CFD/EXP comparison at INCAS WT conditions. M=1.05 with error bars.

For the building of the final aerodynamic database the nominal CFD data are considered, since they cover all the range of Mach number and angle of attack, associated with suitable confidence levels bars. This means that the final uncertainties are the summation of all uncertainties (numerical and experimental) and, if necessary, an enlargement is applied in order to contain the nominal experimental data (as for the pitching moment coefficient).
The following Figure 18 reports the final arrangement for the M=1.05 case.

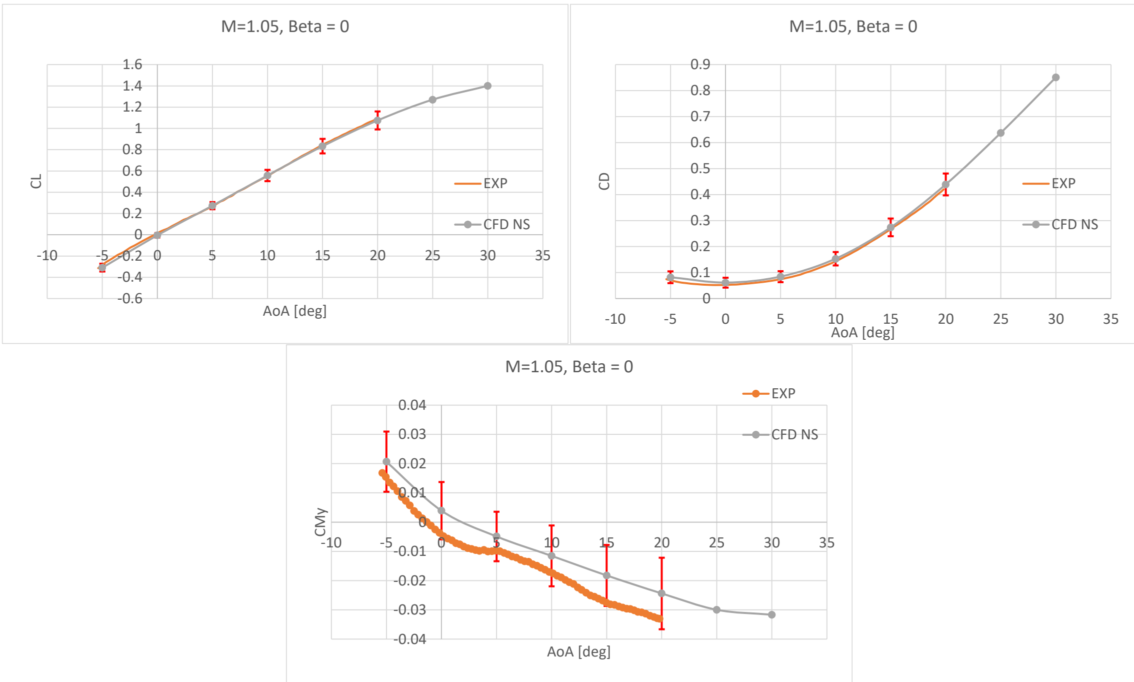

Figure 18 – Final AEDB for M=1.05 with uncertainties bars.

6. Conclusions

This paper reports all the numerical and experimental activities conducted in order to build the aerodatabase of the Case Study CS-2 (REL-HTB test vehicle) in the framework of the H2020 More&Less project. The comparison between CFD data and experimental measurements is of paramount importance for the finalization of database to be used for flight mechanics analyses, and in general for the CS-2 has been very satisfactory. The overall building process of the aerodatabase is described especially for what concerns the uncertainties to be associated to the nominal values. The CFD data that covers all the range of Mach number and angle of attack are used as nominal values and the uncertainties are a summation of all the sources of errors and are suitably built in such a way to include all the data.

7. Contact Author Email Address

mailto: p.roncioni@cira.it

8. Copyright Statement

Acknowledgment

This work has been carried out within the frame of "MDO and REgulations for Low boom and Environmentally Sustainable Supersonic aviation" (MORE&LESS) project. This project has received funding from the European Union's Horizon 2020 research and innovation program under grant agreement No 101006856.

References

[1] https://cordis.europa.eu/project/id/101006856. Accessed 31/01/2022.

[2] Viola, N., et al., "H2020 STRATOFLY Project: from Europe to Australia in less than 3 hours", 32nd Congress of the International Council of the Aeronautical Sciences, Shanghai, CN, 2021.

[3] Viola, N., Roncioni, P., Gori, O., and Fusaro, R., "Aerodynamic Characterization of Hypersonic Transportation Systems and Its Impact on Mission Analysis", Energies, Vol. 14, N. 3590, 2021. https://doi.org/10.3390/en14123580.

[4] Viola, N., Fusaro, R., Gori, O., Marini, M., Roncioni, P., Saccone, G., & Bodmer, D. (2021). STRATOFLY MR3–how to reduce the environmental impact of high-speed transportation. In AIAA SciTech 2021 Forum (p. 1877).

[5] Fusaro, R., Gori, O., Ferretto, D., Viola, N., Roncioni, P. and Marini, M., "Integration of an increasing fidelity aerodynamic modelling approach in the conceptual design of hypersonic cruiser", 32nd Congress of the International Council of the Aeronautical Sciences, Shanghai, CN; 2021.

[6] Fusaro, R., Ferretto, D., Viola, N., "Model-Based Object-Oriented systems engineering methodology for the conceptual design of a hypersonic transportation system", *Proceedings of 2016 IEEE International Symposium on Systems Engineering (ISSE)*, Edinburgh (UK), 2016. https://doi.org/10.1109/SysEng.2016.7753175.

[7] Fusaro, R., Ferretto, D., Viola, N., "MBSE approach to support and formalize mission alternatives generation and selection processes for hypersonic and suborbital transportation systems", *Proceedings of 2017 IEEE International Systems Engineering Symposium (ISSE)*, Vienna (AT), https://doi.org/10.1109/SysEng.2017.8088275.

[8] Goncalves, P. M., Ispir, A. C. and Saracoglu, B. H., Development and optimization of a hypersonic civil aircraft propulsion plant with regenerator system, AIAA Propulsion and Energy 2019 Forum, Indianapolis (IN), USA, 2019 https://doi.org/10.2514/6.2019-4421.

[9] Ferretto, D., Fusaro, R. and Viola, N., A conceptual design tool to support high-speed vehicle design, AIAA Aviation 2020 Forum, 2020 https://doi.org/10.2514/6.2020-2647.

[10] Steelant, J., Varvill, R., Walton, C., Defoort, S., Hannemann, K., & Marini, M. (2015). Achievements obtained for sustained hypersonic flight within the LAPCAT-II project. In 20th AIAA international space planes and hypersonic systems and technologies conference (p. 3677).

[11] Roncioni, P., Rufolo G.C., Votta R., Marini M., An Extrapolation-to-Flight Methodology for Wind Tunnel Measurements Applied to the PRORA-USV FTB1 Vehicle. IAC2006, Valencia, Spain.

[12] Schlichting, H., Boundary Layer Theory, McGRAW-HILL, 1979.

[13] Raymer, D. P., "Aircraft design: a conceptual approach", edited by J. A. Schetz, 6th Edition, AIAA Education Series, AIAA, Reston (VA), 2018. https://doi.org/10.2514/4.104909.

[14] Deng, A., Aerodynamic Performance Prediction of SpaceShipTwo, December 2012, DOI: 10.13140/RG.2.1.354.

[15] Simeonides, G., "The VKI hypersonic wind tunnels and associated measurement techniques," Technical Memorandum VKI TM-46, von Karman Institute for Fluid Dynamics, November 1990.

[16] Cakir, B. O., Grossir, G., Paris, S., and Saracoglu, B. H., "On the design of a Mach 5 axisymmetric contoured nozzle for the VKI H3 hypersonic tunnel," HiSST: 2nd International Conference on High-Speed Vehicle Science Technology (2022).

[17] Gyenge, A., Cakir, B. O., Grossir, G., Saracoglu, B. H., and Chazot, O. "Flow characterization of the Mach 5 hypersonic nozzle of VKI-H3 wind tunnel," AIAA SciTech Forum and Exposition 2024. (2024).

[18] Jivraj, F., Bond, A., Varvill, R., and Paniagua, G., "The scimitar precooled Mach 5 engine," 2007.

[19] Varvill, R., Duran, I., Kirk, A., Langridge, S., Nailard, O., Payne, R., and Webber, H., "Sabre Technology Development Status and Update," 8th European conference for aeronautics and space sciences (EUCASS) (2019).

[20] Durbin, T., Grossir, G. and Chazot, O. "Hypersonic aerodynamic predictions for arbitrary geometries using ANTARES." HiSST: 2nd International Conference on High-Speed Vehicle Science Technology (2022).